Supplement of
Increasing manmade air pollution likely to reduce rainfall in southern West Africa

Pante et al.

In this supplementary information we briefly describe rainfall and aerosol trends for the first rainy season (FRS) in analogy to the results for the Little Dry Season (LDS) and Second Rainy Season (SRS) shown in the main paper.

The optimal linear regression model to describe the relation between rainfall and climate indices (see Section 2.4 in the main paper) is dominated by a simple linear model built on the Atlantic 3 index as in the LDS and SRS, particularly over Ivory Coast (yellow in Supplementary Fig. S1a). In southwestern Ghana and Nigeria there are larger regions showing a higher correlation with the coupled ocean-atmosphere Atlantic Meridional Mode (red), and farther inland Niño3.4 (turquoise) is the most important climate index. At three grid points in the border region of Togo and Benin the combination of the Niño3.4 and Indian Ocean indices (purple) yields the best linear model. This combination does not appear during the LDS and SRS (cf. Fig. 2a, c in the main paper). The resulting correlation coefficients between the optimum linear model and rainfall rarely exceed values of 0.5 (Supplementary Fig. S1b) and thus are generally lower during the FRS than during the LDS and SRS.

Time series of the frequency of relative humidity exceeding 95%, cloud cover, incoming solar radiation, and horizontal visibility during the FRS show very similar behavior as the respective time series of the LDS and the SRS (cf. Supplementary Fig. S2 with Figs. 8 and 11 in the main paper). The relative humidity does not change significantly over the years (Supplementary Fig. S2 top). Increasing values in cloud albedo are clearly anti-correlated with the decreasing radiation time series (Supplementary Fig. S2 middle) and the increase in the category of low horizontal visiblity (Supplementary Fig. S2 bottom) is as evident as during the LDS and the SRS.

Rainfall trends from 1983–2015 during the FRS are positive close to the coastline and in the western part of southern West Africa (Supplementary Fig. ~~S2a~~S3a, b). Further inland and to the east, trends are negative, particularly in the region around Lake Volta. Spatially averaged trends are small and not statistically significant on the 20% level (Supplementary Fig. ~~S2e~~S3c). As correlations with climate indices are rather low (Supplementary Fig. S1b), the differences between the full and residual trends are small. For the more recent trends from 2001–2017 patterns shift, showing positive trends mostly over elevated terrain and negative trends in coastal and lowland regions (Supplementary Fig. ~~S2d~~S3d, e). As seen for the longer period, the spatially averaged trends and the differences between full and residual trends are small (Supplementary Fig. ~~S2f~~S3f).

Trends in aerosol optical depth (AOD) are positive near the coast in the eastern part of the region (Supplementary Fig. ~~S3~~S4). Possible causes are increases in emissions from Nigerian oil fields (i.e., gas-flaring, Deetz & Vogel, 2017) and from the growing coastal cities in the region. Central African fire activity peaks later in the year (Le Page et al., 2010). Since precipitation during

the FRS is dominated by highly organized convective systems (Maranan et al., 2018), aerosol effects are not assumed to have a major impact on rainfall, despite the increasing AOD values in parts of the region.

Trends of the frequency of horizontal visibility observations for the three categories "below 10 km" (bottom), "10–20 km" (middle), and "above 20 km" (top) in % year^{-1} reveal the same evolution for the FRS as for the LDS and the SRS (cf. Supplementary Fig. S5 with Fig. 9 in the main paper). The shift of visibility observations from the medium and high ranges towards the "below 10 km"-category is statistically significant at the $\alpha = 5\%$ level at all stations except Atakpame and Parakou where we find the opposite trend.

References

Deetz, K. & Vogel, B. Development of a new gas-flaring emission dataset for southern West Africa. *Geosci. Model Dev.* **10**, 1607–1620, https://doi.org/10.5194/gmd-10-1607-2017, (2017).

Le Page, Y., Oom, D., Silva, J. M. N., Jönsson, P. & Pereira, J. M. C. Seasonality of vegetation fires as modified by human action: observing the deviation from eco-climatic fire regimes. *Global Ecol. Biogeogr.* **19**, 575–588, https://doi.org/10.1111/j.1466-8238.2010.00525.x, (2010).

Maranan, M., Fink, A. H. & Knippertz, P. Rainfall types over southern West Africa: Objective identification, climatology and synoptic environment. *Q. J. Roy. Meteor. Soc.* **144**, 1628–1648, https://doi.org/10.1002/qj.3345, (2018).

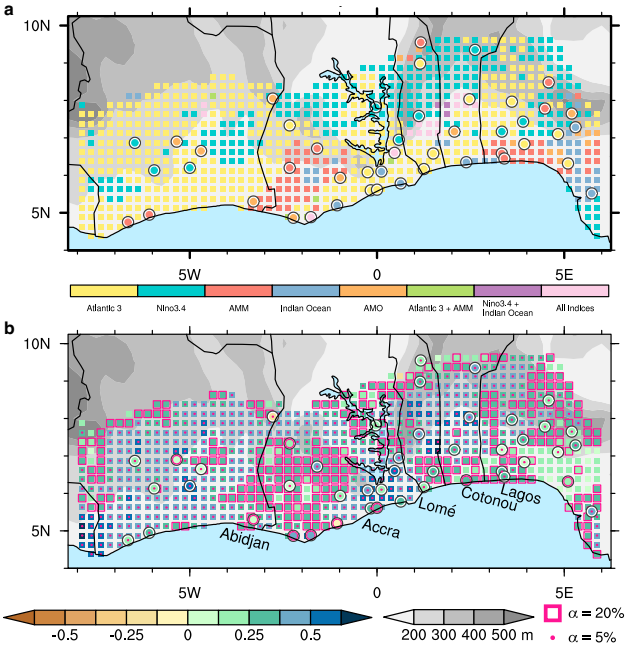

Figure S1. Optimum linear model for the first rainy season (analogous to Fig. 2 in the main paper).

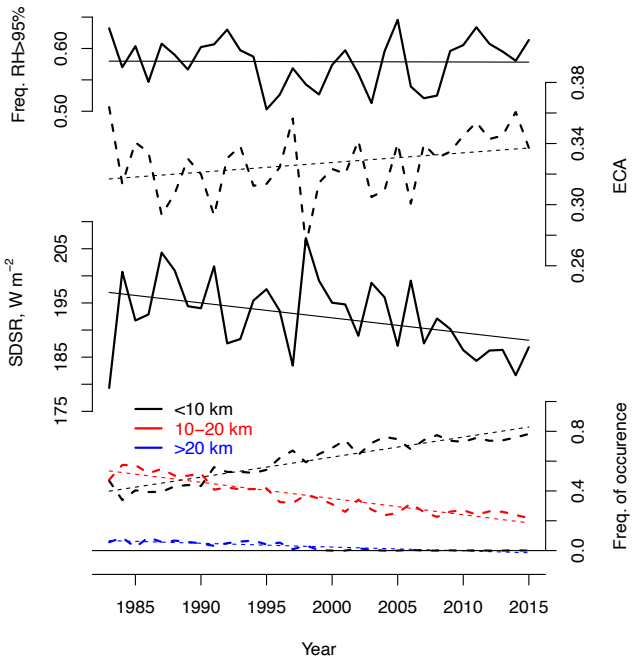

Figure S2. ~~**Rainfall trends for the first rainy season**~~ **Time series for the first rainy season** (analogous to Figs. 4, 8, and ~~5~~ 11 in the main paper).

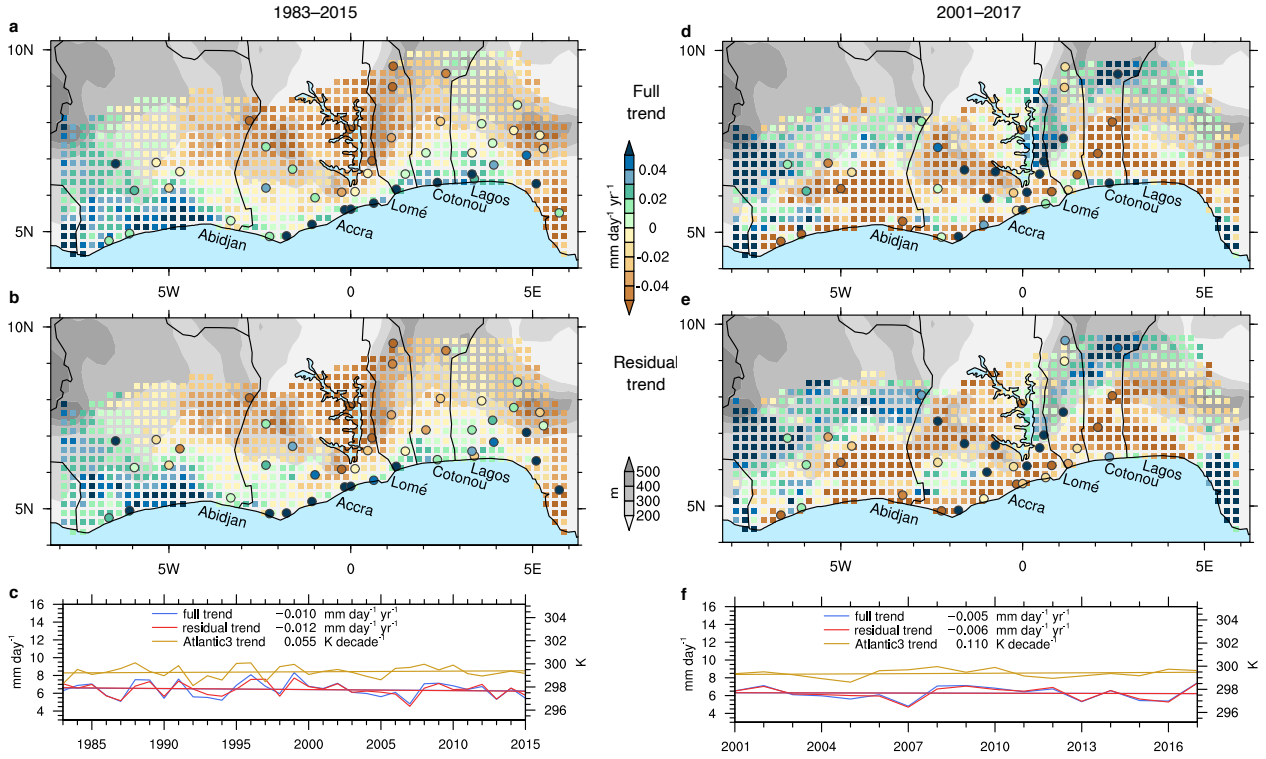

Figure S3. **Rainfall trends for the first rainy season** (analogous to Figs. 5 and 6 in the main paper).

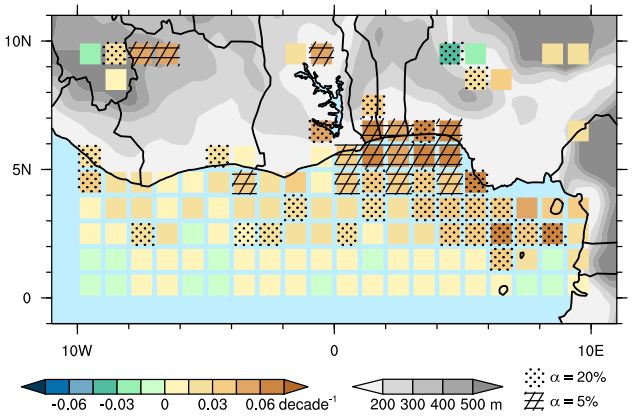

Figure S4. Aerosol optical depth trends for the first rainy season (analogous to Fig. ~~6~~ 7 in the main paper).

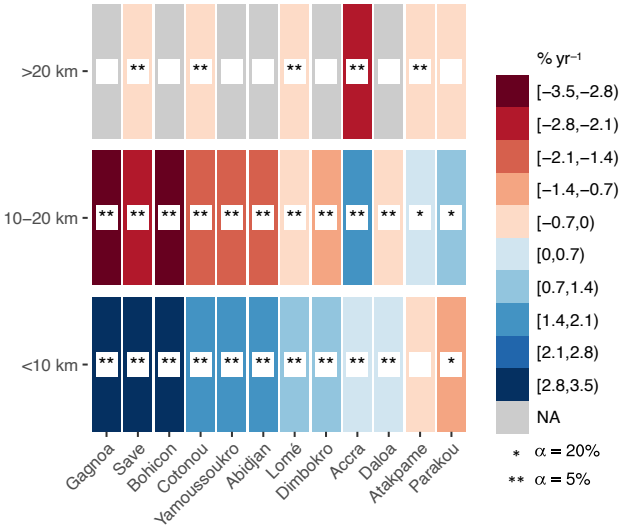

Figure S5. **Visibility trends for the first rainy season** (analogous to Fig. 9 in the main paper).